Adoptive transfer of effector CD8+ T cells derived from central memory cells establishes persistent T cell memory in primates

Carolina Berger,[1] Michael C. Jensen,[2] Peter M. Lansdorp,[3,4] Mike Gough,[5] Carole Elliott,[5] and Stanley R. Riddell[1,6]

[1]Fred Hutchinson Cancer Research Center, Seattle, Washington, USA. [2]Division of Cancer Immunotherapeutics and Tumor Immunology, City of Hope National Medical Center, Duarte, California, USA. [3]Terry Fox Laboratory, British Columbia Cancer Agency, Vancouver, British Columbia, Canada. [4]Department of Medicine, University of British Columbia, Vancouver, British Columbia, Canada. [5]University of Washington National Primate Center, Seattle, Washington, USA. [6]Department of Medicine, University of Washington, Seattle, Washington, USA.

The adoptive transfer of antigen-specific T cells that have been expanded ex vivo is being actively pursued to treat infections and malignancy in humans. The T cell populations that are available for adoptive immunotherapy include both effector memory and central memory cells, and these differ in phenotype, function, and homing. The efficacy of adoptive immunotherapy requires that transferred T cells persist in vivo, but identifying T cells that can reproducibly survive in vivo after they have been numerically expanded by in vitro culture has proven difficult. Here we show that in macaques, antigen-specific CD8+ T cell clones derived from central memory T cells, but not effector memory T cells, persisted long-term in vivo, reacquired phenotypic and functional properties of memory T cells, and occupied memory T cell niches. These results demonstrate that clonally derived CD8+ T cells isolated from central memory T cells are distinct from those derived from effector memory T cells and retain an intrinsic capacity that enables them to survive after adoptive transfer and revert to the memory cell pool. These results could have significant implications for the selection of T cells to expand or to engineer for adoptive immunotherapy of human infections or malignancy.

Introduction

Studies in rodents have demonstrated that adoptive immunotherapy with antigen-specific CD8+ cytotoxic T cells is effective for cancer and infections, and there is evidence that this approach has therapeutic activity in humans (1–8). For clinical applications, T cells of a desired antigen specificity are isolated or engineered to express receptors that target infected or transformed cells and are then expanded in culture (9–14). In some settings the transfer of cloned T cells has been used to provide precise control of specificity and avoid toxicity. For example, in allogeneic stem cell transplantation, the administration of donor-derived T cell clones that target pathogens or malignant cells in the recipient can avoid graft-versus-host disease, which occurs with the infusion of unselected polyclonal donor T cells (3, 4, 15). However, the efficacy of adoptive immunotherapy in humans is often limited by the failure of cultured T cells, particularly cloned CD8+ T cells, to persist in vivo (16, 17), and insight into the basis for the poor survival of the transferred cells is lacking.

The pool of lymphocytes from which CD8+ T cells for adoptive immunotherapy can be derived includes naive T cells (T_N) and antigen-experienced memory T cells (T_M), which can be divided into central memory (T_{CM}) and effector memory (T_{EM}) subsets that differ in phenotype, homing, and function (18). CD8+ T_{CM} express CD62L and CCR7, which promote migration into LNs and proliferate rapidly if reexposed to antigen (19). CD8+ T_{EM} lack CD62L, enabling migration to peripheral tissues, and exhibit immediate effector function (19). In response to antigen stimulation, both CD8+ T_{CM} and T_{EM} proliferate and differentiate into CD62L− cytolytic effector T cells (T_E) that express high levels of granzymes and perforin but are short lived (20). Thus acquisition of an effector phenotype during culture has been suggested as a major reason for the poor survival of transferred T cells (9).

In the normal host, T cell memory persists for life, indicating that some T_M cells may have the ability to self-renew or revert to the memory pool after differentiating to T_E in response to repeated antigen exposure (21). T_{CM} and T_{EM} have distinct phenotypic and functional properties, but it is unknown whether T_E cells derived from each of these T_M subsets retain any intrinsic properties of the parental cell. Using a nonhuman primate model relevant to human translation, we sought to determine whether T_E clones derived from purified T_{CM} or T_{EM} differed in their ability to persist in vivo or establish T cell memory after adoptive transfer. Here we show that antigen-specific CD8+ T_E clones derived from the T_{EM} subset of T_M survive in the blood for only a short duration after adoptive transfer, fail to home to LNs or BM, and do not reacquire phenotypic markers of T_M. By contrast, T_E clones derived from T_{CM} persist long term after adoptive transfer, migrate to T_M niches, reacquire phenotypic properties of T_M, and respond to antigen challenge.

Results

Characterization of CMV-specific CD8+ T cell clones from CD62L+ T_{CM} and CD62L− T_{EM} subsets. Immunocompetent *Macaca nemestrina* with latent CMV infection were used in this study. We identified CMV epitopes recognized by CD8+ T cells in individual macaques by stimulating aliquots of PBMCs with CMV immediate early 1 (IE-1)

Nonstandard abbreviations used: IE, immediate early (protein); ΔLNGFR, intracellular truncated low-affinity nerve growth factor receptor; T-APC, antigen-presenting T cells; T_{CM}, central memory T cells; T_E, effector T cells; T_{EM}, effector memory T cells; T_M, memory T cells; T_N, naive T cells.

Conflict of interest: P.M. Lansdorp is a founding shareholder in Repeat Diagnostic Inc.

Citation for this article: *J. Clin. Invest.* **118**:294–305 (2008). doi:10.1172/JCI32103.

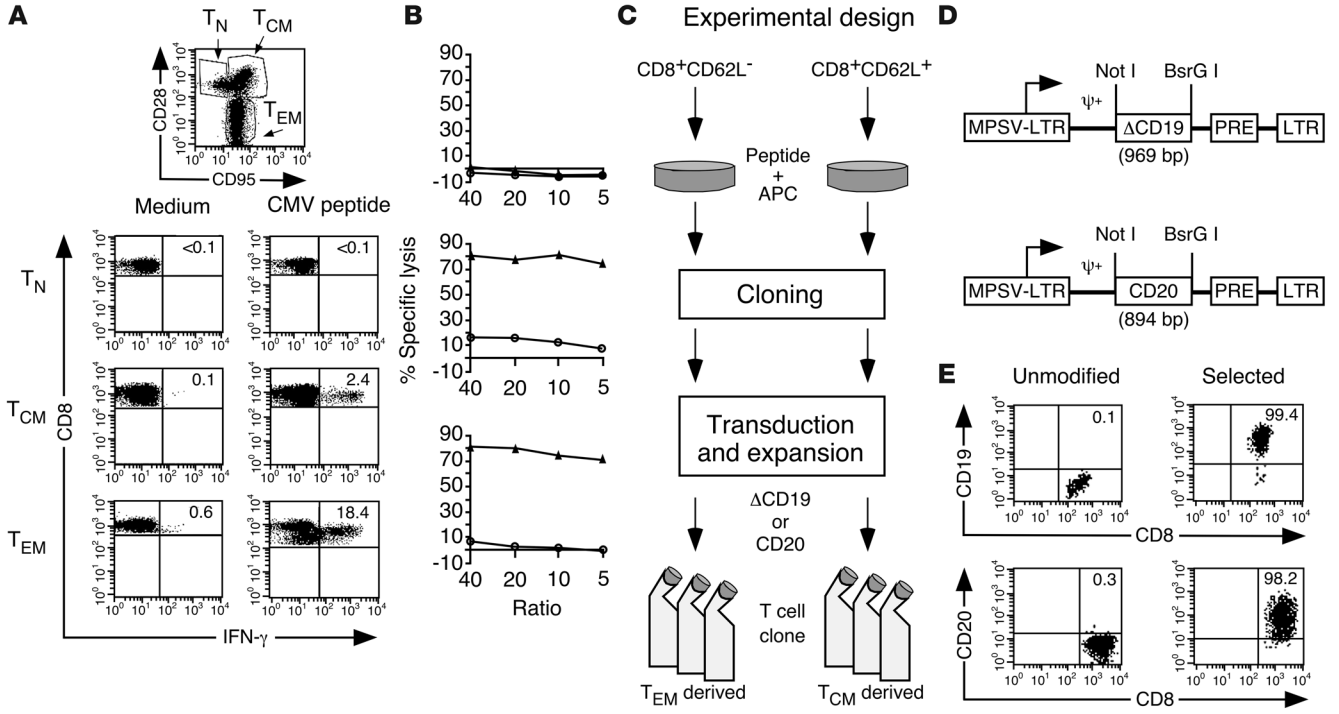

Figure 1

Isolation and gene marking of T_{CM}- and T_{EM}-derived CMV-specific CD8+ T cell clones for adoptive transfer. (**A**) CMV IE-specific T cells are present in T_{CM} and T_{EM} subsets of CD8+ peripheral blood lymphocytes. PBMCs from macaque 02258 were stained with mAbs to CD28, Fas, and CD8 to identify CD28+CD8+Fas^{lo} T_N, CD28+CD8+Fas^{hi} T_{CM}, and CD28–CD8+Fas^{hi} T_{EM} fractions (left panel) and assayed by cytokine flow cytometry after stimulation with a CMV peptide (right panels). (**B**) Sorted CD62L+CD28+CD8+Fas^{lo} T_N (top panel), CD62L+CD28+CD8+ Fas^{hi} T_{CM} (middle panel), and CD62L–CD28–CD8+Fas^{hi} T_{EM} (lower panel) T cells were stimulated with autologous CMV IE peptide-pulsed monocytes and assayed for cytolytic activity against peptide-pulsed (filled triangles) or unpulsed target cells (open circles). (**C**) Isolation of T_{CM}- and T_{EM}-derived CMV-specific CD8+ T cell clones. CD8+CD62L– and CD8+CD62L+ T cell subsets were cultured with peptide-pulsed monocytes. At day 7, T cell clones were isolated by limiting dilution, transduced to express ΔCD19 or CD20, and expanded for adoptive transfer. (**D**) Design of the retroviral vector constructs. MPSV-LTR, myeloproliferative sarcoma virus retroviral long terminal repeat; ψ+, extended packaging signal; PRE, woodchuck hepatitis virus posttranscriptional regulatory element; ΔCD19, truncated macaque CD19 cDNA; CD20, full-length macaque CD20 cDNA. (**E**) Selection of ΔCD19- and CD20-modified CD8+ T cell clones. Transduced T cells were enriched for ΔCD19 or CD20 expression using immunomagnetic beads and analyzed by flow cytometry to assess purity (right panels). Unmodified T cells (left panels) served as control. The percentages of CD8+ T cells positive for CD19 or CD20 are indicated.

or IE-2 peptides and analyzing IFN-γ production by flow cytometry (22). We then determined whether the CD8+ T cells that made IFN-γ after CMV stimulation were present in T_{CM}, T_{EM}, and/or T_N subsets using cytokine flow cytometry after staining with CD8-, CD28-, and CD95 (Fas)–specific mAbs. T_N and T_{CM} are both CD62L+ and CD28+ but can be distinguished from each other by differential expression of Fas, whereas CD62L– T_{EM} can be identified by low or absent CD28 expression (22). T_N did not make IFN-γ after CMV peptide stimulation, and cytolytic T cells were not generated after a single in vitro stimulation with peptide-pulsed monocytes (Figure 1, A and B). By contrast, a subset of T cells in both the T_{CM} and T_{EM} fractions produced IFN-γ after stimulation with CMV peptides, and CMV-specific cytolytic T cells were easily generated from these subsets after stimulation with peptide-pulsed monocytes (Figure 1, A and B).

CD8+ CMV-specific T_E clones were then isolated from 3 macaques by stimulating sorted CD62L+CD8+ and CD62L–CD8+ cells once with peptide-pulsed monocytes, followed by limiting dilution cloning (Figure 1C). We used CD62L rather than Fas and CD28 as the marker for sorting T_{CM} and T_{EM} for cloning to avoid potential effects that binding of Fas or CD28 mAbs in culture might have on T cell differentiation after TCR ligation. Cytolytic CD8+ CMV-specific T cell clones were readily obtained from both CD62L+ and CD62L– subsets in all macaques. The cloning efficiency of plated T cells was 13.6%–23.2% for cultures initiated from T_{CM} and 0.4%–10.4% for cultures initiated from T_{EM}. To permit tracking of the infused cells after adoptive transfer, individual T cell clones from each of the CD62L+ and CD62L– subsets were transduced with a retrovirus encoding either the truncated macaque CD19 (ΔCD19) or CD20 gene and transduced T cells were selected to greater than 95% purity (Figure 1, D and E).

A pair of T_{CM}- and T_{EM}-derived CMV-specific clones was randomly selected for each of 3 macaques and expanded in culture to more than 5×10^9 cells over a total duration of 49 days before adoptive transfer. Independent of their derivation from CD62L+ or CD62L– cells, the T cell clones had differentiated to T_E during culture and had similar phenotypic and functional properties. The T_{CM}- and T_{EM}-derived clones were negative for CD62L, CCR7, CD28, and CD127 and positive for granzyme B and perforin expression (Figure 2A). The deficiency of CD62L expression was confirmed by quantitative RT-PCR (Supplemental Figure 1A; supplemental material available online with this article; doi:10.1172/

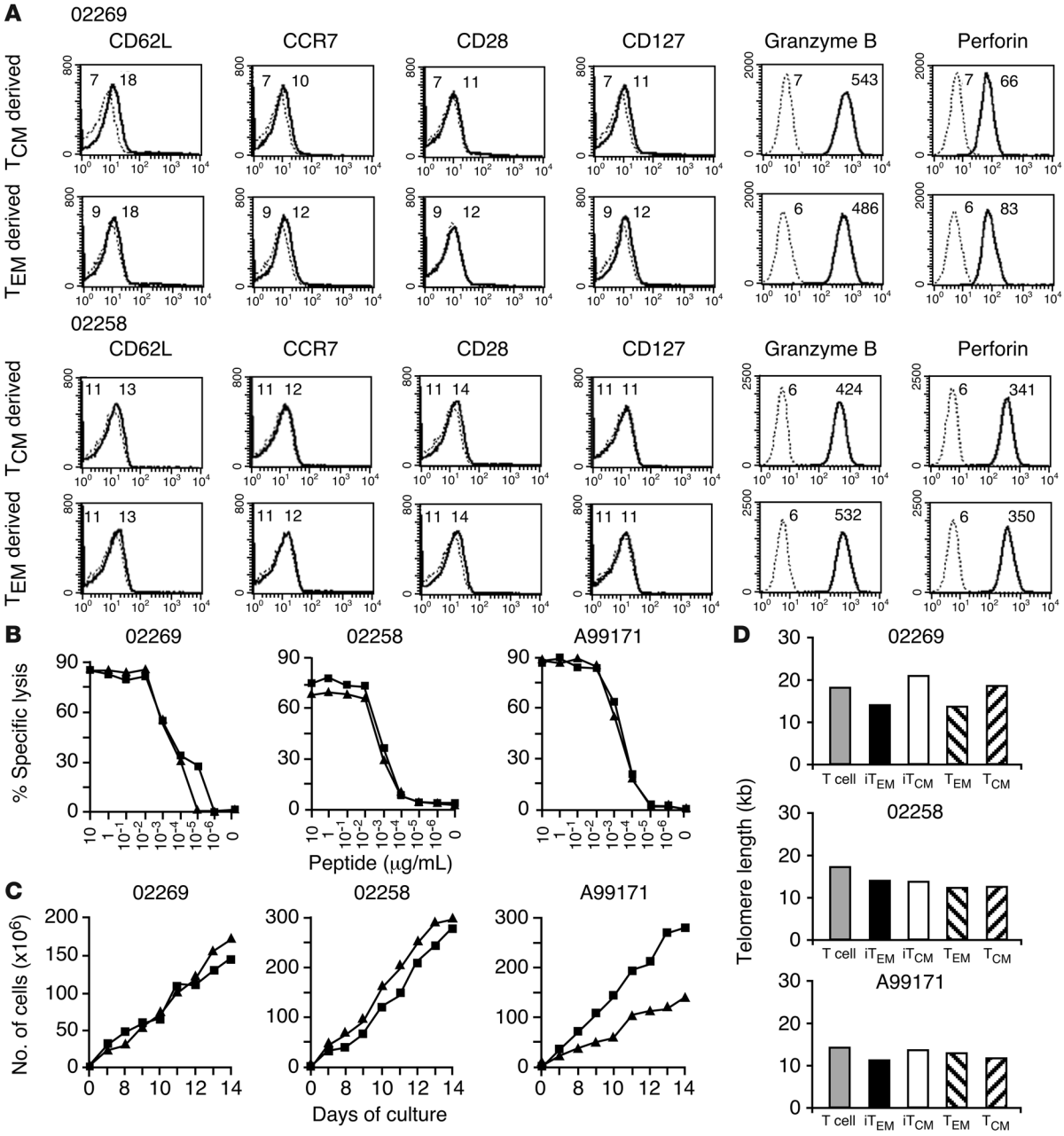

Figure 2

Phenotypic and functional characterization of T_{CM}- and T_{EM}-derived CMV-specific CD8+ T cell clones. (**A**) Expression of CD62L, CCR7, CD28, CD127, granzyme B, and perforin (bold line) on individual T_{CM}- and T_{EM}-derived clones from 2 macaques. The dotted line indicates results from staining with an isotype control. Inset values represent the MFI. The data are shown for pairs of T_E clones used for adoptive transfer in macaques 02269 and 02258 and is representative of data for all clones used for adoptive transfer. (**B**) Cytotoxic activity of each pair of T_{EM}-derived (filled triangles) and T_{CM}-derived (filled squares) clones was examined at an effector-to-target ratio (E/T ratio) of 20:1 using autologous peptide-pulsed target cells. The peptide sequences were KKGDIKDRV (macaque 02269), ATTRSLEYK (macaque 02258), and EEHVKLFFK (macaque A99171). (**C**) In vitro growth of CMV-specific CD8+ T cell clones. T_{EM}-derived (filled triangles) and T_{CM}-derived (filled squares) clones used for adoptive transfer were stimulated with anti-CD3 and anti-CD28 mAbs, γ-irradiated feeder cells, and IL-2 (50 U/ml), and cell growth was measured by counting viable cells. (**D**) Telomere length in T_{CM}- and T_{EM}-derived CMV-specific T cell clones. The median telomere length of duplicate samples was measured by automated flow-FISH in peripheral blood T lymphocytes, in the infused T cell clones (iT_{EM} and iT_{CM}), and in each of 2 additional randomly selected T_{EM}- and T_{CM}-derived T cell clones from each macaque.

JCI32103DS1). The T_{CM}- and T_{EM}-derived clones expressed a high level of CXCR4 and a low level of CD26, both of which may be involved in regulating cell migration to the BM (Supplemental Figure 1, B and C) (23, 24). The T cell clones of each pair recognized the same CMV peptide and had similar proliferation kinetics (Figure 2, B and C). Because telomere length was reported to

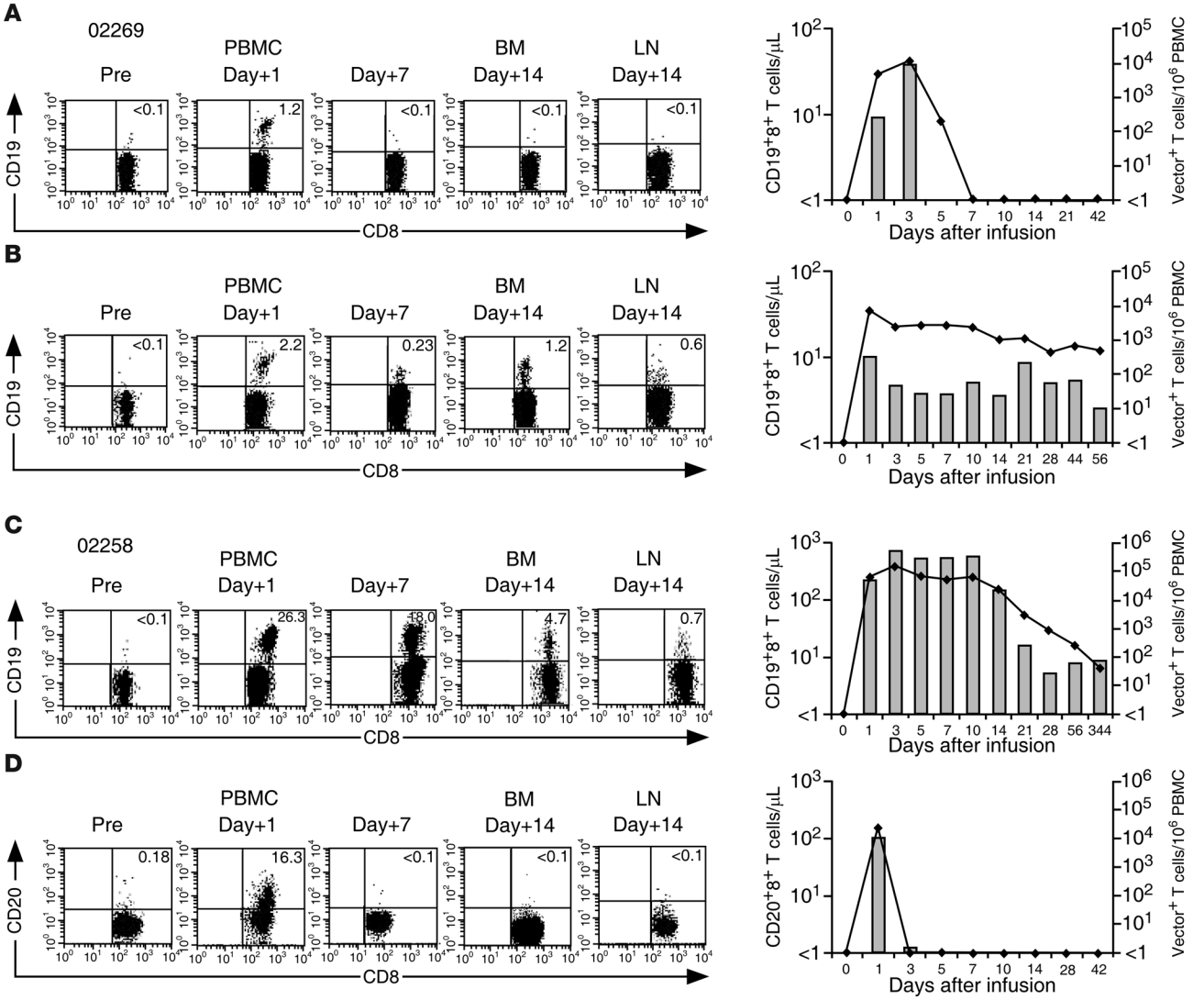

Figure 3

Persistence and migration of T_{EM}- and T_{CM}-derived $CD8^+$ T_E clones in PBMCs, BM, and LNs following adoptive transfer. (**A** and **B**) ΔCD19-modified T_{EM}-derived (**A**) and T_{CM}-derived (**B**) clones were transferred to macaque 02269 in separate infusions at a cell dose of 3×10^8/kg, and samples of PBMCs, BM, and LNs were collected before (pre) and at the indicated times following infusion. The frequency of transferred $CD19^+$ T cells was determined by flow cytometry and by PCR for vector sequences. Left: Percentage of $CD19^+CD8^+$ T cells by flow cytometry in PBMCs, BM, and LNs before and after infusion of the T_{EM}-derived (**A**) and T_{CM}-derived (**B**) clones. Cells were gated on $CD3^+CD8^+$ T cells. Right: Absolute numbers of $CD19^+CD8^+$ T cells/μl of blood determined by flow cytometry (gray bars; left *y* axis) and vector-positive T cells/10^6 PBMCs (filled diamonds; right *y* axis). (**C** and **D**) ΔCD19-modified T_{CM}-derived and CD20-modified T_{EM}-derived clones were transferred to macaque 02258 in separate infusions at a cell dose of 6×10^8/kg. Aliquots of blood, BM, and LNs obtained at the indicated times were analyzed by flow cytometry and PCR to detect transferred $CD19^+CD8^+$ (**C**) or $CD20^+CD8^+$ (**D**) cells, respectively. Left: Percentage of $CD8^+$ T cells that expressed ΔCD19 (**C**) or CD20 (**D**) in PBMCs, BM, and LNs. Cells were gated on $CD3^+CD8^+$ T cells. Right: Absolute number of marked $CD8^+$ T cells/μl of blood (gray bars; left *y* axis) and vector-positive T cells/10^6 PBMCs (filled diamonds; right *y* axis).

correlate with in vivo persistence of transferred T cells in a prior study (25), we measured the telomere lengths of each clone using automated FISH and flow cytometry (flow-FISH), and although there was some variation, telomere length was not significantly different between T_{EM}- and T_{CM}-derived clones (Figure 2D).

In vivo persistence of $CD8^+$ T_E clones derived from T_{CM} or T_{EM}. We administered the autologous gene-modified T cells intravenously and measured their frequency in the blood, LNs, and BM at intervals after infusion. The BM is known to be a niche for T_M and contains hematopoietic progenitor cells, which are a major site of latent CMV infection (26). A T_{EM}-derived ΔCD19-modified T cell clone was transferred to macaque 02269 at a dose of 3×10^8 T cells/kg, which is approximately 5%–10% of the macaque total lymphocyte pool (27). $CD19^+CD8^+$ T cells were detected in the blood 1 day after the infusion at a frequency of 1.2% of $CD8^+$ cells or 10 cells/μl of blood. The $CD19^+$ T cells peaked in the blood at 3.7% of $CD8^+$ T cells (40 cells/μl) on day 3 after infusion. However, transferred T cells were not detected in blood at day 5 or at multiple check points up to 42 days after infusion, or in BM or LN samples obtained 14 days after infusion (Figure 3A). PCR to amplify retroviral vec-

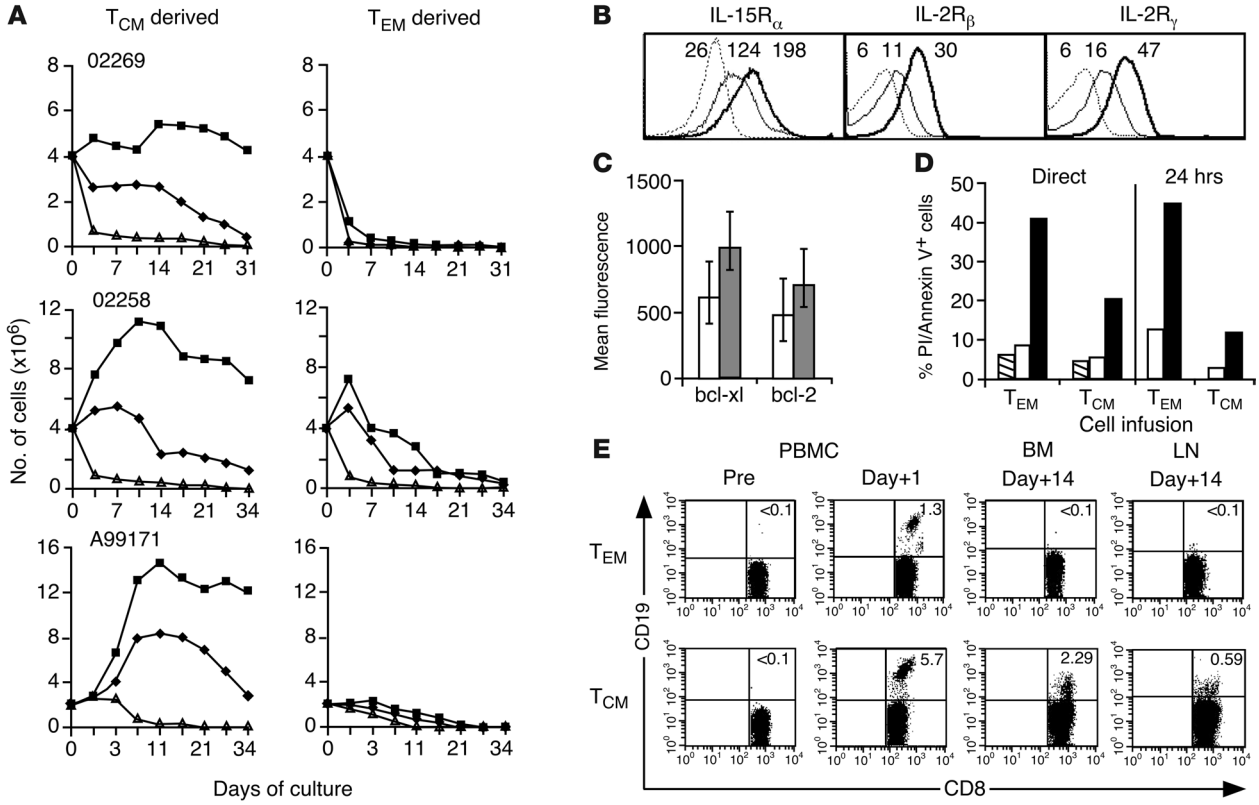

Figure 4

CD8$^+$ T_{CM}-derived clones exhibit improved survival in IL-15 in vitro and decreased apoptosis in vivo. (**A**) Aliquots of T_{EM}- and T_{CM}-derived clones used for adoptive transfer were plated at the end of a 14-day stimulation cycle in medium alone (open triangles), IL-2 (1 ng/ml) (filled diamonds), or IL-15 (1 ng/ml) (filled squares), and viability was determined using Trypan blue dye exclusion. Data are representative of 13 T_{CM}- and 11 T_{EM}-derived clones from 3 macaques. (**B**) Expression of IL-15Rα, IL-2Rβ, and IL-2Rγ on T_{CM}-derived (bold lines) and T_{EM}-derived (black lines) clones transferred to macaque 02269 was measured by flow cytometry on days 13–14 after stimulation (dotted lines, isotype control mAb). Data are representative of clones administered to macaques 02258 and A99171. (**C**) Bcl-xl and Bcl-2 expression on 3 T_{EM}-derived (white bars) and T_{CM}-derived (gray bars) clones transferred to macaques 02269, 02258, and A99171 analyzed 14 days after stimulation. Mean ± SD of the MFI is shown on the *y* axis. (**D**) Apoptosis of T_{EM}- and T_{CM}-derived clones in vivo. The percent of CD19$^+$CD8$^+$ T cells in PBMCs that were Annexin V$^+$ and/or PI$^+$ 1 day after infusion of ΔCD19$^+$ T_{EM}-derived or T_{CM}-derived T cell clones to macaque A99171 was determined directly and after 24-hour culture. Samples were gated on CD8$^+$CD19$^-$ (white bars) and CD8$^+$CD19$^+$ T cells (black bars). Hatched bars show the T cells used for infusion. (**E**) Persistence and migration of T_{EM}-derived and T_{CM}-derived T_E clones in macaque A99171. PBMC, BM, and LN cells obtained at indicated times were analyzed by flow cytometry to detect transferred CD19$^+$CD8$^+$ T_E in samples gated on CD3$^+$CD8$^+$.

tor sequences in DNA from peripheral blood, BM, and LNs confirmed the absence of the transferred T cells (Figure 3A and data not shown). We transferred the same dose of a ΔCD19-modified T cell clone derived from the T_{CM} subset to this macaque. One day after infusion, the frequency of CD19$^+$CD8$^+$ T cells in the blood was 2.2% of CD8$^+$ T cells (10 cells/μl), but in contrast to the T_{EM}-derived clone, the T_{CM}-derived cells persisted in the blood for longer than 56 days at approximately 0.2% of CD8$^+$ T cells (3–6 cells/μl) and comprised 1.2% and 0.6% of CD8$^+$ T cells in BM and LN samples, respectively, obtained 14 days after the infusion (Figure 3B).

In the second macaque (macaque 02258), we infused a higher cell dose (6×10^8/kg) and gave a ΔCD19-modified T_{CM}-derived clone first. With this dose, the transferred cells were detected in the blood at a frequency of 26.3% of CD8$^+$ T cells (228 cells/μl) on day 1 and 46.3% of CD8$^+$ T cells (734 cells/μl) on day 3. The transferred T_{CM}-derived clone was also detected in the BM and LN samples obtained on day 14 at 4.7% and 0.7% of CD8$^+$ T cells, respectively (Figure 3C). The frequency of the transferred cells in the blood declined gradually over 28 days to 7–10 cells/μl but remained detectable by flow cytometry and PCR for more than 11 months after infusion (Figure 3C). The second infusion in this animal consisted of the same dose of a T_{EM}-derived clone transduced with the CD20 retrovirus to enable the cells to be distinguished from the previously transferred ΔCD19-modified clone. The frequency of CD20$^+$CD8$^+$ T cells in the blood 1 day after the infusion was 16.3% of CD8$^+$ T cells (103 cells/μl), but the transferred cells were not detected in the blood at day 5 or in BM and LN samples obtained on day 14 (Figure 3D). The disappearance of CD20-modified T cells was confirmed by PCR for vector sequences on DNA from samples of PBMCs, BM, and LNs (Figure 3D and data not shown).

CD8$^+$ T_E cells derived from T_{CM} are rescued from cytokine withdrawal in vitro by IL-15 and undergo less apoptosis in vivo after adoptive transfer. The failure of T_E clones derived from T_{EM} to persist after adoptive transfer could be due to cell death in vivo and/or rapid migration to tissue sites other than blood, LNs, or BM. We compared the in vitro survival of multiple T_{CM}- and T_{EM}-derived clones after cul-

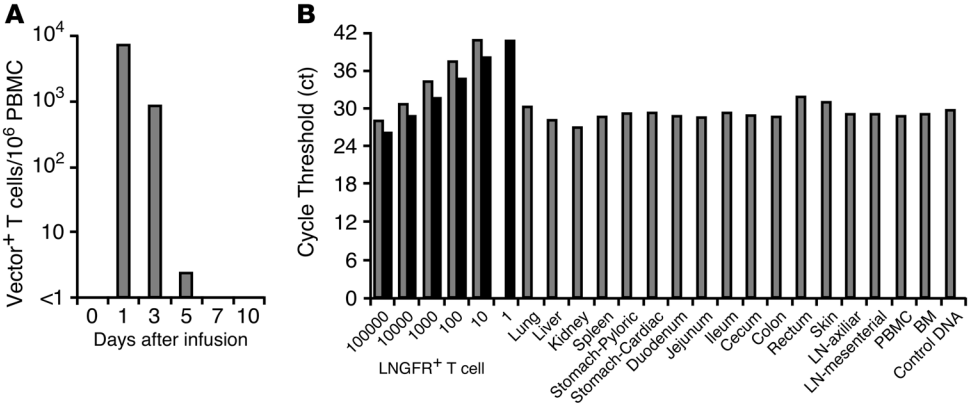

Figure 5

Persistence and migration of a T_{EM}-derived $CD8^+$ T_E clone in PBMCs and tissue sites following adoptive transfer. (**A**) Persistence and migration of a ΔLNGFR-modified T_{EM}-derived T cell clone in PBMCs. The $\Delta LNGFR^+$ T cell clone was transferred at a cell dose of 6×10^8/kg. Aliquots of blood were collected at the indicated times and analyzed by PCR for the frequency of transferred $\Delta LNGFR^+$ T cells. Shown are the absolute numbers of vector-positive T cells/10^6 PBMCs (gray bars) before and at intervals after infusion. (**B**) A necropsy was performed on day 10 after the T cell infusion. Samples of DNA were isolated from various tissues as indicated and examined for the presence of the transferred vector-positive cells (black bars) using a real-time PCR assay. DNA isolated from $\Delta LNGFR^+$ T cells was serially diluted 1:10 in water prior to amplification with the appropriate primer set. The real-time PCR assay to detect β-actin (gray bars) was used as a control to detect genomic DNA. The threshold cycle is shown for each sample.

ture in media alone or in media containing cytokines such as IL-7 and IL-15 that maintain endogenous $CD8^+$ T_M (28–30). T_{EM}- and T_{CM}-derived T_E clones lacked expression of IL-7 receptor-α (IL-7Rα) (CD127; Figure 2A) and died within 14 days when cultured in media alone or with IL-7 (Figure 4A and data not shown). Culture in IL-15 or IL-2 at doses of 1 ng/ml slightly prolonged the survival of some T_{EM}-derived clones, but the cell number declined by more than 70% over 17 days (Figure 4A). By contrast, T_{CM}-derived clones increased or maintained cell number for over 30 days when cultured in 1 ng/ml of IL-15 and exhibited improved survival in IL-2 (Figure 4A). Even a low dose of IL-15 (100 pg/ml) was sufficient to maintain the cell number of T_{CM}-derived clones for longer than 21 days (data not shown). The ability of IL-15 to promote the survival of T_{CM}-derived but not T_{EM}-derived clones correlated with higher levels of IL-15Rα, IL-2Rβ, and IL-2Rγ expression (Figure 4B).

T_{EM}-derived T cell clones expressed lower levels of Bcl-xl and Bcl-2 than T_{CM}-derived clones (Figure 4C) and died rapidly in vitro even when exposed to cytokines that promote T cell survival, suggesting these T cells may be more susceptible to apoptosis in vivo. Therefore, we infused a ΔCD19-modified T_{EM}-derived T cell clone to a third macaque (macaque A99171) and directly measured the proportion of transferred cells undergoing apoptosis in vivo by PI staining and Annexin V binding (31). The T_{EM}-derived clone did not show significant levels of PI staining or Annexin V binding immediately prior to infusion and was detected in PBMCs at greater than 1% of $CD8^+$ T cells on day 1 after infusion. However, approximately 40% of the $CD19^+CD8^+$ cells in the day 1 PBMC sample were PI and/or Annexin V positive. To ensure that Annexin V binding to exposed phosphatidylserine was not transient due to stress from infusion, an aliquot of PBMC obtained on day 1 was placed into culture for 24 hours and staining with PI and Annexin V was repeated. After 24 hours of culture, the proportion of $CD19^+CD8^+$ T cells that were PI and/or Annexin V positive had increased to 45% (Figure 4D). As observed in prior macaques, the transferred $CD19^+$ T cells were not detected in PBMC obtained on day 5 or in the BM or LN samples obtained on day 14 by flow cytometry or PCR for vector sequences (Figure 4E and data not shown). We then infused a ΔCD19-modified T_{CM}-derived clone into the same animal and analyzed the proportion of infused cells that underwent apoptosis. On day 1, greater than 5% of $CD8^+$ T cells were $CD19^+$ and less than 20% were PI and/or Annexin V positive, both on direct analysis of PBMC and after 24 hours of culture (Figure 4D). As observed in prior animals, the T_{CM}-derived clone migrated to the BM and LNs and persisted in the blood for more than 4 months (Figure 4E and data not shown). The difference in persistence of T_{CM}-derived and T_{EM}-derived clones in the 3 macaques was significant ($P < 0.03$).

To address the possibility that a small proportion of transferred T_{EM} might migrate to and persist only in tissue sites, we performed a necropsy on 1 macaque 10 days after the infusion of a T_{EM}-derived clone. In this experiment, the intracellular truncated low-affinity nerve growth factor receptor (ΔLNGFR) was used as a marker to allow the cells to be distinguished from previously infused ΔCD19- and CD20-marked T cells. As observed with prior infusions, the T_{EM}-derived T cells were detected in the blood on day 1 at 7,376 $\Delta LNGFR^+$ cells/10^6 PBMCs (27 cells/μl) but declined rapidly and were not detected after day 5 (Figure 5A). DNA was prepared from samples of lung, liver, kidney, stomach, small intestine, large intestine, skin, spleen, LNs, and BM obtained on day 10 and analyzed for ΔLNGFR vector sequences and for β-actin by real-time PCR. We did not detect ΔLNGFR-marked T cells in any tissue from this animal (Figure 5B). Together with the high levels of apoptosis in vivo after the infusion of T_{EM}-derived clones, this data suggests that the lack of persistence of T_{EM}-derived T cells in the blood reflects cell death rather than sequestration in tissues.

Adoptively transferred $CD8^+$ T_E clones derived from T_{CM} acquire a memory phenotype in vivo. CD62L was not expressed by $CD8^+$ T_{CM}-derived T_E clones at the time of adoptive transfer by flow cytometry, and we did not observe reexpression of CD62L when the T_{CM}-derived clones were cultured in vitro with IL-2 or IL-15 (Figure 2A). However, the observation that the transferred T_{CM}-derived cells migrated to LNs in all 3 animals suggested that CD62L might be reexpressed in vivo. CD62L was not expressed during the brief period the T_{EM}-derived clones persisted in the blood in any of the macaques, but as early as 3 days after each infusion of T_{CM}-derived T_E, a subset of the transferred cells in PBMC were $CD62L^+$ (Figure 6A). $CD62L^+CD19^+$ T cells were also present in BM and LNs obtained 14 and 56 days after the infusions of T_{CM}-derived clones (Figure 6, A and B). The proportion of transferred cells that were $CD62L^+$ in the LNs was greater than in blood or BM (Figure 6B).

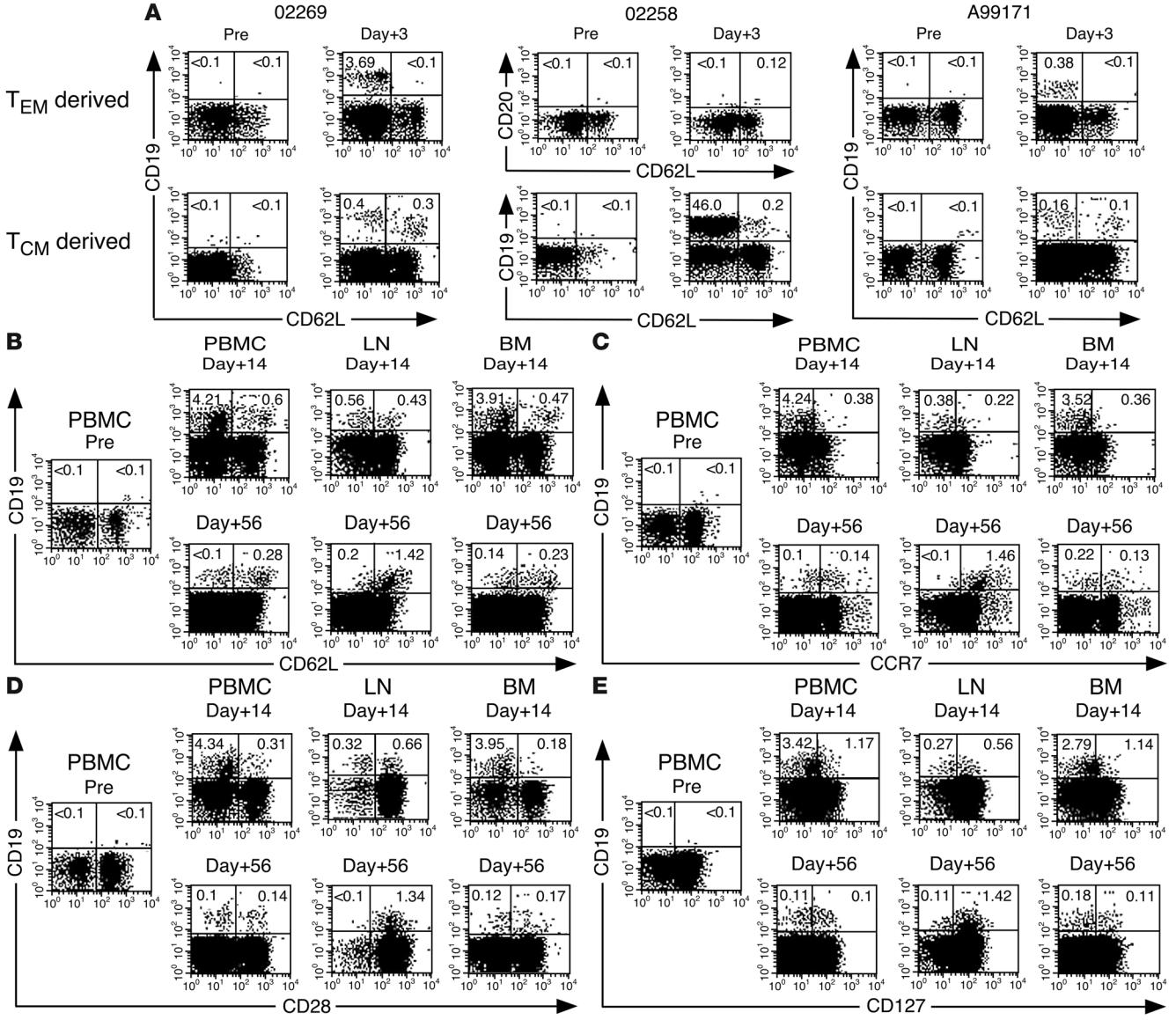

Figure 6

Adoptively transferred T_{CM}-derived T_E reexpress markers of T_{CM} in vivo and persist in memory cell niches. (**A**) Expression of CD62L on T_{EM}-derived (upper panels) or T_{CM}-derived (lower panels) T_E clones after adoptive transfer. Samples of PBMCs were obtained before and on day 3 after the infusion of T_{CM}- and T_{EM}-derived clones and analyzed by flow cytometry after gating on $CD3^+CD8^+$ T cells. The percentage of T cells that expressed the ΔCD19 or CD20 marker gene and CD62L is shown in the upper right quadrant of each panel. (**B**–**E**) A major fraction of $CD8^+$ T cells that persist after adoptive transfer acquire phenotypic markers of T_{CM} and reside in LNs. Aliquots of PBMCs, LNs, and BM were obtained from macaque 02258 at days 14 and 56 after infusion of the ΔCD19-modified T_{CM}-derived clone. The expression of phenotypic markers of T_{CM}, including CD62L (**B**), CCR7 (**C**), CD28 (**D**), and CD127 (**E**) on the subset of transferred $CD19^+$ T cells was determined by flow cytometry after gating on $CD3^+CD8^+$ cells.

The expression of $CD62L^+$ on transferred T cells after infusion prompted us to examine whether other memory markers were acquired that were absent on the infused T_E. A subset of the $CD19^+CD8^+$ T cells in PBMC and LNs obtained 14 days after transfer expressed CCR7, CD28, and CD127 (Figure 6, C–E). This analysis was repeated on samples obtained 56 days after cell transfer in macaque 02258. At this later time, the transferred $CD19^+CD8^+$ T cells now comprised 1.4% of all $CD8^+$ T cells in the LNs, and these cells were uniformly positive for markers of T_{CM} including CD62L, CCR7, CD28, and CD127 (Figure 6, B–E). Transferred T cells were present at lower levels in PBMC and BM than in LNs and contained both $CD62L^+$ and $CD62L^-$ fractions. Thus despite expansion and differentiation of a single T_{CM} cell to more than 5×10^9 T_E cells, a significant fraction of the cells were able to persist long term after adoptive transfer, revert their phenotype to that of T_{CM}, and compete with endogenous T cells to occupy anatomical niches of T_{CM}.

T cells established by adoptive transfer exhibit functional properties of both T_{CM} and T_{EM}. We next examined whether the $CD62L^+$ and $CD62L^-$ CMV-specific T cells established by adoptive transfer were functional and had properties of T_{CM} and T_{EM}. Stimula-

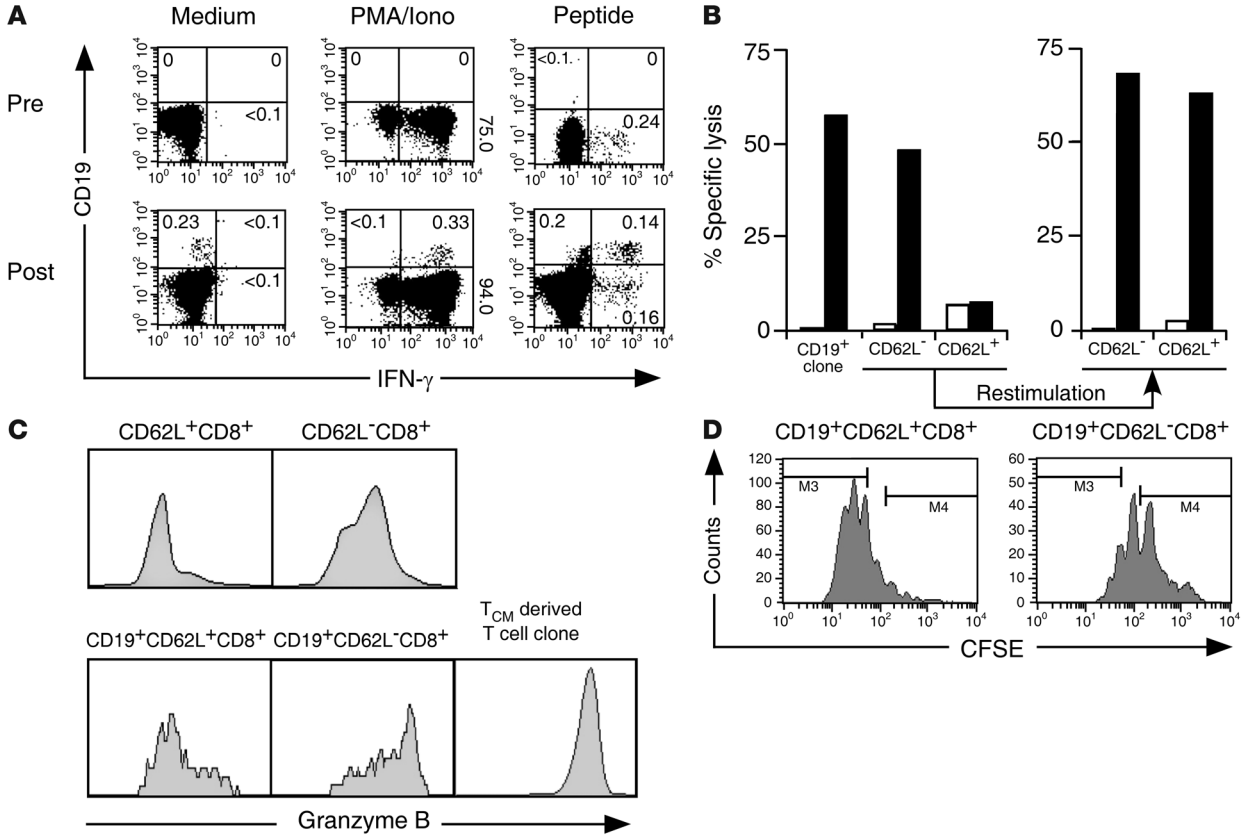

Figure 7

Adoptively transferred CD8+ T cells exhibit functional properties of T_M. (**A**) IFN-γ production. PBMCs obtained from macaque 02269 before and 14 days following infusion of a ΔCD19+ CMV-specific T cell clone were stimulated with medium, PMA/ionomycin, or peptide antigen and examined by cytokine flow cytometry. Data are gated on CD3+CD8+ cells and are representative of results from macaque 02258. (**B**) Transferred T cells that reexpress CD62L lack direct cytotoxicity but acquire cytotoxic function after stimulation. Left: PBMCs obtained 14–70 days after infusion of a T_{CM}-derived CD19+CD8+ clone to macaque 02258 were pooled, sorted into CD19+CD62L−CD8+ and CD19+CD62L+CD8+ fractions (purity >80%), and examined for lysis of autologous unpulsed (white bars) or peptide-pulsed target cells (black bars) (E/T ratio, 5:1). The cultured T_{CM}-derived ΔCD19+CD8+ clone served as positive control for lysis. Right: Sorted CD19+CD62L−CD8+ and CD19+CD62L+CD8+ T cells were stimulated using anti-CD3 and anti-CD28 mAbs for 14 days and then assayed for lysis of peptide-pulsed target cells (E/T ratio, 5:1). (**C**) Granzyme B expression. PBMCs and the transferred T_{CM}-derived clone were stained with mAbs to CD62L, CD8, and CD19 as well as intracellular granzyme B. Cells were analyzed by flow cytometry after gating on CD62L+CD8+, CD62L−CD8+, CD19+CD62L+CD8+, and CD19+CD62L−CD8+ cells. (**D**) Proliferation. PBMCs obtained from macaque 02269 on days 14–70 after infusion were sorted into CD19+CD62L+CD8+ (left panel) and CD19+CD62L−CD8+ subsets (right panel), labeled with CFSE, and stimulated with peptide-pulsed APCs as described in Methods. After 5 days, CFSE dilution was assessed by flow cytometry after gating on CD19+CD3+CD8+ cells. M3 gate, proportion of cells that have undergone more than 5 divisions.

tion of PBMC with the cognate peptide induced IFN-γ production by the CD19+CD8+ cells, and the frequency of responding cells was comparable to that of endogenous CD19− CMV-specific CD8+ T cells (Figure 7A). To measure cytolytic function, we pooled blood samples from multiple time points to obtain sufficient cells to sort CD19+CD62L+CD8+ and CD19+CD62L−CD8+ fractions and assayed lysis of peptide-pulsed target cells. The CD19+CD62L− subset had cytolytic activity nearly equivalent to that of the infused T cell clone and expressed granzyme B at levels comparable to endogenous CD62L−CD8+ T cells (Figure 7, B and C). The CD19+CD62L+ subset lacked direct cytolytic activity and had lower granzyme B expression, but in vitro stimulation of the CD19+CD62L+ T cells induced differentiation to cytolytic effector cells (Figure 7, B and C). To assess proliferative capacity, we labeled an aliquot of the sorted CD19+CD62L+ and CD19+CD62L− T cells with CFSE and monitored dye dilution 5 days after peptide stimulation. Five ore more cell divisions were found in 74% of the CD62L+CD19+ cells, but only in 13% of CD62L−CD19+ cells (Figure 7D).

CMV is latent in macaques, and reactivation is rare in immunocompetent hosts. Thus to determine whether the T_M established by adoptive transfer could respond to antigen stimulation in vivo, we infused autologous T cells pulsed with CMV IE peptide (forming antigen-presenting T cells [T-APC]). We chose to use T-APCs because these cells could be easily prepared and prior human studies have shown that T cells expressing a foreign antigen can boost antigen-specific T_M responses in vitro and in vivo (32, 33). Peptide-pulsed T-APCs were lysed by the CMV-specific T cell clone in vitro (Figure 8A) and were infused to macaque A99171 nine weeks after transfer of the CD19+ T_{CM}-derived clone. Seven days after the T-APC infusion, there was a 4- to 5-fold increase in the absolute numbers of both ΔCD19-modified T cells and

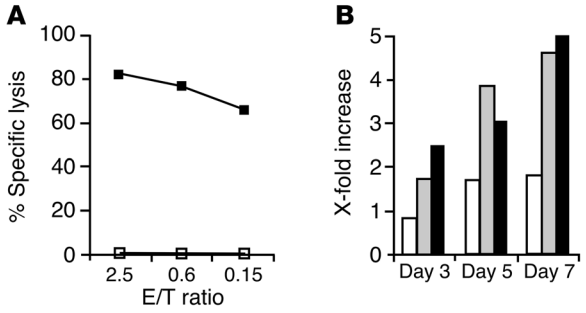

Figure 8

Adoptively transferred T cells expand in vivo to antigen stimulation. (**A**) T-APCs pulsed with IE peptide are lysed by IE-specific $CD8^+$ T cells. T-APCs generated from macaque A99171 were pulsed with peptide (filled squares) or media alone (open squares), labeled with ^{51}Chromium, and used as targets for the autologous IE-specific $CD8^+$ T cell clone that was used for adoptive transfer. (**B**) Expansion of endogenous and transferred CMV-specific T cells by infusion of T-APCs. A dose of 1×10^7 T-APCs/kg was administered to macaque A99171 nine weeks after infusion of a $CD19^+$ T_{CM}-derived clone. The number of $CD3^+CD8^+$ T cells and $CD19^+CD8^+$ T cells/μl of blood was measured by flow cytometry prior to and on indicated days following the T-APC administration. The number of endogenous IE-specific $CD8^+$ T cells was measured by cytokine flow cytometry at the same time points after gating on $CD19^-CD3^+CD8^+$ cells. The data show the fold increase in the absolute numbers of $CD3^+CD8^+$ T cells (white bars), $CD19^+CD8^+$ T cells (gray bars), and $CD19^-$ IE-specific $CD8^+$ T cells (black bars) after the T-APC infusion.

endogenous CMV IE-1–specific T cells in PBMC (Figure 8B). The infusion of T-APCs in macaque 02258 also resulted in an increase in absolute number of a previously transferred $\Delta CD19^+$ T_{CM}-derived clone in the blood (5.8-fold), while previously administered $CD20^+$ T_{EM} remained undetectable after the T-APC infusion (data not shown). Thus T_M established by adoptive transfer were capable of responding to antigen in vivo.

Discussion

The inability of adoptively transferred T cells to persist in vivo has correlated with a lack of efficacy in clinical trials of adoptive immunotherapy for infections and cancer and has been suggested to result from differentiation during in vitro culture (9, 16, 17). The persistence and antitumor efficacy of cultured T cells used for therapy of cancer can sometimes be improved by depletion of host lymphocytes before cell transfer to eliminate regulatory cells and competition for cytokines and by the administration of IL-2 after cell transfer (6, 17). However, these interventions do not uniformly improve the persistence of transferred T cells, suggesting that intrinsic properties of T cells that are isolated for adoptive therapy may be an additional determinant of their fate in vivo. Here we show in a nonhuman primate model that antigen-specific $CD8^+$ T_E clones derived from T_{CM} but not T_{EM} precursors are able to persist long term, migrate to T_M niches, and acquire phenotypic and functional properties of T_{CM} after adoptive transfer.

After encountering antigen in vivo, T cells undergo proliferation and programmed differentiation evoked by signals from the TCRs, costimulatory and adhesion molecules, and cytokine receptors (18, 20, 34). These events generate large numbers of T_E that die as antigen is cleared and a smaller pool of phenotypically distinct T_{CM} and T_{EM} that respond to antigen reexposure by differentiating into T_E. Data from both murine and human studies support a linear differentiation model in which T_{CM} give rise to both T_{EM} and T_E, although it remains possible that T_{CM} and T_{EM} represent separate lineages (18, 35–37). The capacity of T cell memory to be maintained for life suggests that at least some T_M are capable of both self-renewal and differentiation (21).

Our study derived and expanded antigen-specific T cell clones from purified T_{CM} and T_{EM} and transferred these cells back into normal macaques without prior lymphodepletion or cytokine administration after cell transfer. In contrast to clinical trials of adoptive T cell therapy, where it is not possible to conclusively distinguish the transferred T cells from endogenous cells of the identical antigen and TCR specificity from which they were derived, we used gene marking to enable precise detection of transferred T cells. Although similar in function, phenotype, and proliferation before infusion, T cell clones derived from T_{CM} or T_{EM} exhibited remarkably different fates in vivo. T_{CM}-derived clones persisted long term in the blood, migrated to LNs and BM, and underwent phenotypic conversion to both T_{CM} and T_{EM} after adoptive transfer. T_{EM}-derived clones consistently failed to persist in the blood longer than 5 days and were not detected in LNs or BM. The demise of T_{EM}-derived clones correlated with higher levels of apoptosis immediately after cell transfer, and a necropsy at day 10 after transferring a T_{EM}-derived clone failed to detect these cells in any tissue site. Additional experiments analyzing T cell migration to tissues at earlier time points might provide further insight into the fate of T_{EM}-derived clones. We chose to use culture conditions that are highly efficient and used commonly for propagating human T cells for clinical immunotherapy. Both T_{CM}- and T_{EM}-derived clones proliferated equivalently well in vitro, but we cannot exclude the possibility that alternative culture conditions might yield cells with improved engraftment properties or that alterations to the host environment before or after transfer might enable T_{EM} clones to persist.

A notable difference between T_{CM}- and T_{EM}-derived clones was the ability of IL-15, a γ_c cytokine required for maintenance of $CD8^+$ T_M (28, 29), to prevent apoptotic cell death after cytokine withdrawal. IL-15, which can directly bind to IL-15Rα on T cells or be transpresented by IL-15Rα–bearing cells (38), may be the initial stimulus that enables survival of T_{CM}-derived cells in vivo, although the later acquisition of IL-7Rα on transferred T cells is consistent with a role for IL-7 in the reversion of T_E to long-lived T_{CM} (39). Gene expression and epigenetic profiling may provide further insight into the basis for the marked differences in the survival of T_E clones derived from T_{CM} and T_{EM} and the ability of T_{CM}-derived clones to reacquire phenotypic and functional properties of T_{CM} (40, 41).

A prior study attempted to recapitulate in vivo programming of T_{CM} and T_{EM} by a single in vitro stimulation of naive tumor-specific $CD8^+$ T cells from TCR-transgenic mice with antigen and either IL-2 to generate T_{EM} or IL-15 to generate T_{CM} (42). T cells cultured in IL-15 retained CD62L, migrated to LNs, and were more effective in therapy in a murine model of melanoma. It remains to be determined whether the improved survival reflected incomplete differentiation of the T cells during the short-term in vitro culture in IL-15 or true programming of T_{CM} in vitro. It is also unclear whether these properties would be retained through T cell cloning or the multiple cycles of stimulation that are necessary to generate polyclonal T cells for clinical immunotherapy from rare human tumor-specific or virus-specific T_N precursors.

Our discovery that T_E cells derived as clonal populations from T_{CM} are capable of reexpressing molecules required for homing to lymphoid organs and establishing reservoirs of functional T_{CM} and T_{EM} in vivo has implications for the selection of T cells for adoptive immunotherapy of viral diseases and cancer (1–8). For example, the results suggest that the durability of immune reconstitution achieved by adoptive transfer of donor virus-specific T cells to allogeneic stem cell transplant recipients would be improved by ensuring that T cells are expanded for therapy from the $CD62L^+$ T_{CM} subset of the donor. Because virus-specific $CD62L^+$ T_{CM} are typically present in lower frequency than T_{EM} in the blood, selection of T_{CM} cells prior to in vitro expansion would ensure that the cell product consisted of T_E cells that were able to persist and revert to the memory pool. The isolation of tumor-reactive T cells from cancer patients is difficult due to their low frequency and/or functional impairments in the tumor-bearing host (43, 44). Thus alternative approaches for generating autologous tumor-reactive T cells for cancer therapy have been developed, including the introduction of genes encoding TCRs specific for tumor antigens or chimeric immunoreceptors that target tumor cell surface molecules (11–14, 45). The results presented here suggest that isolating T_{CM} for insertion of genes that encode receptors for molecules on tumor cells may provide a tumor-reactive T cell population with an improved capacity to persist after adoptive transfer.

Methods

Animals and T cell transfer. Adult *M. nemestrina* were housed at the University of Washington National Primate Research Center under American Association for Accreditation of Laboratory Animal Care approved conditions. The Institutional Animal Care and Use Committee of the University of Washington approved the experimental protocols. Healthy macaques with a $CD8^+$ T cell response to CMV IE-1 or IE-2 peptides were selected for the study (22). CMV-specific $CD8^+$ T cell clones were infused intravenously at cell doses of 3×10^8 to 6×10^8/kg. Accredited clinical laboratories performed complete blood counts and serum chemistry. All macaques were followed for at least 8 weeks after each T cell infusion. The persistence of transferred T_{EM}- and T_{CM}-derived clones in the blood was measured by flow cytometry and PCR and compared using the log-rank test.

Retroviral vectors. A truncated macaque CD19 gene encoding for the extracellular and transmembrane domain (ΔCD19) and 4 aa of the cytoplasmic tail to abrogate signaling and the full-length CD20 gene were amplified by RT-PCR and cloned into the retroviral plasmid $pMP71_{pre}$ (a gift from W. Uckert, Max-Delbrück-Center, Berlin, Germany) (46). Retrovirus supernatant was produced in Phoenix Galv packaging cells (a gift from G. Nolan, Stanford University School of Medicine, Stanford, California, USA). A retroviral vector (LV'V) containing ΔLNGFR as a cell surface marker has been described previously (47).

Epitope mapping. Cytokine flow cytometry was used to detect $CD8^+$ T cells in PBMCs that expressed intracellular IFN-γ after stimulation with 24 pools of 15-mer overlapping peptides (NMI) arranged in an analytical grid and spanning the 558 aa rhesus CMV IE-1 protein sequence (GenBank accession no. M93360), or with an IE-2 peptide (a gift of L. Picker, Oregon Health & Science University, Beaverton, Oregon, USA) (22, 32). Immunogenic CMV peptides were identified by the responses of $CD8^+$ T cells to intersecting peptides in the grid, and assays were repeated with each individual peptide and derivative 9-mer peptides to map specificity.

Flow cytometry and cell sorting. T cell clones and PBMCs were analyzed by flow cytometry after staining with fluorochrome-conjugated mAbs to CD3 (SP34), CD4, CD8, CD28, CD62L, CCR7, CD95, CD122 (IL-2Rβ), CD132 (IL-2Rγ), CXCR4, CD26 (BD), CD19, CD8β, and CD127 (Immunotech Coulter), IL-15Rα (R&D), and a secondary mouse IgG_{2B} mAb (BD). For intracellular staining, cells were permeabilized using Cytofix/Cytoperm and stained with mAbs to granzyme B (BD), perforin (Kamiya Biomedical), Bcl-2 (BD), and Bcl-xl (Southern Biotech). Isotype-matched mAbs served as controls. In some experiments, samples were stained with Annexin V–phycoerythrin and PI according to the manufacturer's instructions (BD). Samples were analyzed on a FACSCalibur using CellQuest Software (BD).

For sorting T cell subsets, PBMCs were stained with fluorochrome-conjugated anti-CD8, anti-CD28, and anti-Fas mAbs or with anti-CD8 and anti-CD62L mAbs and sorted using a Vantage BD cell sorter.

Culture and gene marking of CMV-specific T cell clones. Sort-purified $CD8^+CD62L^+$ and $CD8^+CD62L^-$ T cells containing T_{CM} and T_{EM}, respectively, were cocultured with autologous monocytes pulsed with CMV IE-1 or IE-2 peptides (1 μg/ml) in RPMI 1640 supplemented with 25 mM HEPES, L-glutamine, 25 μM 2-mercaptoethanol (all from Invitrogen), and 10% human serum (Gemini; T cell media). IL-2 (10 U/ml; Chiron) was added on day 3. On day 7, T cells were replated at 0.3 cells/well in 96-well round-bottom plates with 1×10^5 γ-irradiated autologous peptide-pulsed PBMCs and 1×10^4 γ-irradiated B-lymphoblastoid lymphocytes in T cell media with 50 U/ml IL-2. After 12–14 days, aliquots from wells with visible growth were tested for recognition of ^{51}Chromium-labeled peptide-pulsed or unpulsed target cells. CMV-specific T cell clones were stimulated with anti-CD3 and anti-CD28 mAbs, human γ-irradiated PBMCs and B-lymphoblastoid lymphocytes, and IL-2 (50 U/ml), as previously described (48, 49). On day 2, cells were exposed to ΔCD19 or CD20 retrovirus supernatant with IL-2 (50 U/ml) and polybrene (5 μg/ml; Chemicon), centrifuged at 1,000 *g* for 1 hour at 32°C, and incubated overnight. The cells were then washed and cultured in T cell media containing IL-2 and on day 8 selected for ΔCD19 or CD20 expression by immunomagnetic selection (Miltenyi Biotec). Cells were cryopreserved in aliquots and thawed subsequently for in vitro expansion for adoptive transfer as previously described (48, 49). The clonality of each infused T cell clone was confirmed by TCR-Vβ gene rearrangement analysis.

Cell viability assays. Aliquots of T cell clones at the end of the 14-day stimulation were plated at 2×10^6 to 4×10^6 cells/well in T cell media alone or with IL-2 (1 ng/ml or 16 U/ml; Chiron), IL-15 (1 ng/ml; R&D Systems), or IL-7 (10 ng/ml; R&D). Viability was assessed every 3–4 days by Trypan blue dye exclusion.

Cytotoxicity assays. Cytotoxic responses of CMV-specific T cells were examined as described (47–49). Briefly, autologous ^{51}Chromium-labeled T cells were pulsed overnight with peptide antigen at various concentrations or with medium alone and used as targets for $CD8^+$ T cell clones in a chromium-release assay.

Telomere length analysis. The average length of telomere repeats in individual lymphocytes was measured by automated flow-FISH (50, 51). Cryopreserved cells were thawed, hybridized with or without 0.3 μg/ml telomere-specific fluorescein isothiocyanate-conjugated $(CCCTAA)_3$ PNA probe, washed, and counterstained with 0.01 μg/ml LDS 751 (Exciton Chemical). To convert the fluorescence measured in sample cells hybridized with the telomere PNA probe into kilobytes of telomere repeats, fixed bovine thymocytes with known telomere length were used as internal control (51).

CFSE labeling of T cells. Sorted $CD19^+CD62L^+CD8^+$ and $CD19^+CD62L^-CD8^+$ T cells were purified from PBMCs obtained after adoptive transfer and labeled with 0.625 μM CFSE (Invitrogen) in PBS for 10 minutes at 37°C and blocked with 20% FCS medium. CFSE-labeled T cells were plated at 1×10^5 cells/well in a 96-well plate with autologous CD40L-activated B cells (2.5×10^4 cells/well) pulsed with 200 ng/ml cognate peptide. CFSE dilution was analyzed by flow cytometry after 5 days.

PCR. PCR amplifications were performed using a quantitative PCR assay (49). DNA (0.3–1 μg) was amplified in duplicate using PCR primers and TaqMan probes (Applied Biosystems) designed to detect a unique sequence

encompassing the junction of either the CD20 or CD19 gene and the retroviral vector pMP71$_{pre}$. Standards consisted of DNA derived from the infused CD19- or CD20-modified T cell clones. Aliquots of preinfusion PBMCs served as a negative control. PCR to detect the ΔLNGFR vector was performed as described previously (47).

The *M. nemestrina* CD62L was cloned and sequenced, and a quantitative RT-PCR assay was used to determine the expression of CD62L in T cells. Briefly, total RNA was isolated from PBMCs and T cell clones using RNeasy Minikit (Qiagen) and used as template to prepare cDNA by reverse transcriptase (Superscript II; Invitrogen) following the manufacturer's instructions. PCR was carried out in quadruplicate using a SYBR Green kit (Applied Biosystems) for 40 cycles in an ABI Prism 7700 Sequence Detector using SDS software 2.2.2 (Applied Biosystems). The GAPDH gene was used as a standard to correct for RNA quantity and quality. The expression level of CD62L was normalized to that of GAPDH and compared between PBMCs and T cell clones (ABI).

Preparation of T-APCs. Autologous T-APCs were expanded by stimulation with anti-CD3 and anti-CD28 mAbs and IL-2 (50 U/ml). After 14 days, T cells were harvested, pulsed for 90 min with CMV peptide (1 μg/ml), washed twice, and administered intravenously at a cell dose of 1×10^7 to 1×10^8/kg.

Acknowledgments

We thank Irma Vulto (Terry Fox Laboratory) and Michael Berger (Fred Hutchinson Cancer Research Center) for excellent assistance. We thank Louis Picker (Oregon Health & Science University, Beaverton, Oregon, USA) for the IE peptide and helpful discussions. We also thank Peter Barry (University of California Davis, Davis, California, USA). This work was supported by NIH grants R01CA114536 and U01HL66947 (to S.R. Riddell and C. Berger); R01AI053193, CA18029, and M01RR00037 (to S.R. Riddell); and P30CA33572-21, CA30206-25A1, and CA107399-04 (to M.C. Jensen). This work was also supported by Canadian Institutes of Health Research grants MOP38075 and GMH79042 (to P.M. Lansdorp).

Received for publication March 12, 2007, and accepted in revised form October 3, 2007.

Address correspondence to: Carolina Berger, Fred Hutchinson Cancer Research Center, Immunology Program, 1100 Fairview Ave. North, D3-100, Seattle, Washington 98109-1024, USA. Phone: (206) 667-4772; Fax: (206) 667-7983; E-mail: cberger@fhcrc.org.

1. Cheever, M.A., Greenberg, P.D., and Fefer, A. 1980. Specificity of adoptive chemoimmunotherapy of established syngeneic tumors. *J. Immunol.* **125**:711–714.
2. Pahl-Seibert, M.-F., et al. 2005. Highly protective in vivo function of cytomegalovirus IE1 epitope-specific memory CD8 T cells purified by T-cell receptor-based cell sorting. *J. Virol.* **79**:5400–5413.
3. Riddell, S.R., et al. 1992. Restoration of viral immunity in immunodeficient humans by the adoptive transfer of T cell clones. *Science.* **257**:238–241.
4. Walter, E.A., et al. 1995. Reconstitution of cellular immunity against cytomegalovirus in recipients of allogeneic bone marrow by transfer of T-cell clones from the donor. *N. Engl. J. Med.* **333**:1038–1044.
5. Rooney, C.M., et al. 1998. Infusion of cytotoxic T cells for the prevention and treatment of Epstein-Barr virus-induced lymphoma in allogeneic transplant recipients. *Blood.* **92**:1549–1555.
6. Dudley, M.E., et al. 2002. Cancer regression and autoimmunity in patients after clonal repopulation with antitumor lymphocytes. *Science.* **298**:850–854.
7. Bollard, C.M., et al. 2004. Cytotoxic T lymphocyte therapy for Epstein-Barr virus$^+$ Hodgkin's disease. *J. Exp. Med.* **200**:1623–1633.
8. Dudley, M.E., et al. 2005. Adoptive cell transfer therapy following non-myeloablative but lymphodepleting chemotherapy for the treatment of patients with refractory metastatic melanoma. *J. Clin. Oncol.* **23**:2346–2357.
9. Gattinoni, L., et al. 2006. Adoptive immunotherapy for cancer: building on success. *Nat. Rev. Immunol.* **6**:383–393.
10. Blattman, J.N., and Greenberg, P.D. 2004. Cancer Immunotherapy: A treatment for the masses. *Science.* **305**:200–205.
11. Kessels, H.W.H.G., et al. 2001. Immunotherapy through TCR gene transfer. *Nat. Immunol.* **2**:957–961.
12. Stanislawski, T., et al. 2001. Circumventing tolerance to a human MDM2-derived tumor antigen by TCR gene transfer. *Nat. Immunol.* **2**:962–970.
13. Brentjens, R.J., et al. 2003. Eradication of systemic B-cell tumors by genetically targeted human T lymphocytes co-stimulated by CD80 and interleukin-15. *Nat. Med.* **9**:279–286.
14. Morgan, R.A., et al. 2006. Cancer regression in patients after transfer of genetically engineered lymphocytes. *Science.* **314**:126–129.
15. Bleakley, M., and Riddell, S.R. 2004. Molecules and mechanisms of the graft-versus-leukemia effect. *Nat. Rev. Cancer.* **4**:371–380.
16. Dudley, M.E., et al. 2001. Adoptive transfer of cloned melanoma-reactive T lymphocytes for the treatment of patients with metastatic melanoma. *J. Immunother.* **24**:363–373.
17. Yee, C., et al. 2002. Adoptive T cell therapy using antigen-specific CD8$^+$ T cell clones for the treatment of patients with metastatic melanoma: In vivo persistence, migration, and antitumor effect of transferred cells. *Proc. Natl. Acad. Sci. U. S. A.* **99**:16168–16173.
18. Sallusto, F., Geginat, J., and Lanzavecchia, A. 2004. Central memory and effector memory T cell subsets: function, generation, and maintenance. *Annu. Rev. Immunol.* **22**:745–763.
19. Butcher, E.C., and Picker, L.J. 1996. Lymphocyte homing and homeostasis. *Science.* **272**:60–66.
20. Wherry, E.J., et al. 2003. Lineage relationship and protective immunity of memory CD8 T cell subsets. *Nat. Immunol.* **4**:225–234.
21. Fearon, D.T., Manders, P., and Wagner, S.D. 2001. Arrested differentiation, the self-renewing memory lymphocyte, and vaccination. *Science.* **293**:248–250.
22. Pitcher, C.J., et al. 2002. Development and homeostasis of T cell memory in rhesus macaque. *J. Immunol.* **168**:29–43.
23. Peled, A., et al. 1999. Dependence of human stem cell engraftment and repopulation of NOD/SCID mice on CXCR4. *Science.* **283**:845–848.
24. Christopherson, K.W., II, et al. 2004. Modulation of hematopoietic stem cell homing and engraftment by CD26. *Science.* **305**:1000–1003.
25. Zhou, J., et al. 2005. Telomere length of transferred lymphocytes correlates with in vivo persistence and tumor regression in melanoma pateints receiving cell transfer therapy. *J. Immunol.* **175**:7046–7052.
26. Kondo, K., Kaneshima, H., and Mocarski, E.S. 1994. Human cytomegalovirus latent infection of granulocyte-macrophage progenitors. *Proc. Natl. Acad. Sci. U. S. A.* **91**:11879–11883.
27. Sopper, S., et al. 2003. Impact of simian immunodeficiency virus (SIV) infection on lymphocyte numbers and T-cell turnover in different organs of rhesus monkeys. *Blood.* **101**:1213–1219.
28. Schluns, K.S., et al. 2002. Requirement for IL-15 in the generation of primary and memory antigen-specific CD8 T cells. *J. Immunol.* **168**:4827–4831.
29. Becker, T.C., et al. 2002. Interleukin 15 is required for proliferative renewal of virus-specific memory CD8 T cells. *J. Exp. Med.* **195**:1541–1548.
30. Marks-Konczalik, J., et al. 2000. IL-2-induced activation-induced cell death is inhibited in IL-15 transgenic mice. *Proc. Natl. Acad. Sci. U. S. A.* **97**:11445–11450.
31. Vermes, I., et al. 1995. A novel assay for apoptosis. Flow cytometric detection of phosphatidylserine expression on early apoptotic cells using fluorescein labelled Annexin V. *J. Immunol. Methods.* **184**:39–51.
32. Berger, C., et al. 2006. Analysis of transgene-specific immune responses that limit the in vivo persistence of adoptively transferred HSV-TK-modified donor T cells after allogeneic hematopoietic cell transplantation. *Blood.* **107**:2294–2302.
33. Wyss-Coray, T., et al. 1993. Antigen-presenting human T cells and antigen-presenting B cells induce a similar cytokine profile in specific T cell clones. *Eur. J. Immunol.* **23**:3350–3357.
34. Masopust, D., et al. 2004. The role of programming in memory T-cell development. *Curr. Opin. Immunol.* **16**:217–225.
35. Appay, V., et al. 2002. Memory CD8$^+$ T cells vary in differentiation phenotype in different persistent virus infections. *Nat. Med.* **8**:379–385.
36. Marzo, A.L., et al. 2005. Initial T cell frequency dictates memory CD8$^+$ T cell lineage commitment. *Nat. Immunol.* **6**:793–799.
37. Lefrançois, L. and Marzo, A. 2006. The descent of memory T-cell subsets. *Nat. Rev. Immunol.* **6**:618–623.
38. Sato, N., et al. 2007. The IL-15/IL15α on cell surfaces enables sustained IL-15 activity and contributes to the long survival of CD8 memory T cells. *Proc. Natl. Acad. Sci. U. S. A.* **104**:588–593.
39. Kaech, S.M., et al. 2003. Selective expression of the interleukin 7 receptor identifies effector CD8 T cells that give rise to long-lived memory cells. *Nat. Immunol.* **4**:1191–1198.
40. Willinger, T., et al. 2005. Molecular signatures distinguish human central memory from effector memory CD8 T cell subsets. *J. Immunol.* **175**:5895–5903.
41. Wilson, C.B., and Merkenschlager, M. 2006. Chromatin structure and gene regulation in T cell development and function. *Curr. Opin. Immunol.* **18**:143–151.
42. Klebanoff, C.A., et al. 2005. Central memory self/tumor-reactive CD8$^+$ T cells confer superior antitumor immunity compared with effector memory T cells. *Proc. Natl. Acad. Sci. U. S. A.* **102**:9571–9576.
43. Lee, P.P., et al. 1999. Characterization of circulat-

ing T cells specific for tumor-associated antigens in melanoma patients. *Nat. Med.* **5**:677–685.
44. Groh, V., et al. 2002. Tumour-derived soluble MIC ligands impair expression of NKG2D and T-cell activation. *Nature.* **419**:734–738.
45. Sadelain, M., Rivière, I., and Brentjens, R.J. 2003. Targeting tumours with genetically enhanced T lymphocytes. *Nat. Rev. Cancer.* **3**:35–45.
46. Engels, B., et al. 2003. Retroviral vectors for high-level transgene expression in T lymphocytes. *Hum. Gene Ther.* **14**:1155–1168.
47. Berger, C., et al. 2004. Pharmacologically regulated Fas-mediated death of adoptively transferred T cells in a nonhuman primate model. *Blood.* **103**:1261–1269.
48. Riddell, S.R., et al. 1996. T-cell mediated rejection of gene-modified HIV-specific cytotoxic T lymphocytes in HIV-infected patients. *Nat. Med.* **2**:216–223.
49. Berger, C., et al. 2001. Nonmyeloablative immunosuppressive regimen prolongs in vivo persistence of gene-modified autologous T cells in a nonhuman primate model. *J. Virol.* **75**:799–808.
50. Rufer, N., et al. 1998. Telomere length dynamics in human lymphocyte subpopulations measured by flow cytometry. *Nat. Biotechnol.* **16**:743–747.
51. Baerlocher, G.M., and Lansdorp, P.M. 2003. Telomere length measurements in leukocyte subsets by automated multicolor flow-FISH. *Cytometry A.* **55**:1–6.